Atmos. Meas. Tech. Discuss., 5, 8161–8187, 2012
www.atmos-meas-tech-discuss.net/5/8161/2012/
doi:10.5194/amtd-5-8161-2012

Atmospheric Measurement Techniques Discussions

A novel rocket-based in-situ collection technique for mesospheric and stratospheric aerosol particles

W. Reid[1], P. Achtert[2], N. Ivchenko[1], P. Magnusson[1], T. Kuremyr[1], V. Shepenkov[3], and G. Tibert[3]

[1]School of Electrical Engineering, Royal Institute of Technology (KTH), Stockholm, Sweden
[2]Department of Meteorology, Stockholm University, Stockholm, Sweden
[3]Department of Mechanics, Royal Institute of Technology (KTH), Stockholm, Sweden

Received: 27 September 2012 – Accepted: 17 October 2012 – Published: 5 November 2012

Correspondence to: N. Ivchenko (nickolay@kth.se)

Published by Copernicus Publications on behalf of the European Geosciences Union.

Abstract

A technique for collecting aerosol particles between altitudes of 85 and 17 km is described. Collection probes are ejected from a sounding rocket allowing for multi-point measurements. Each probe is equipped with 110 collection samples that are 3 mm in diameter. The collection samples are one of three types: standard transmission electron microscopy carbon grids, glass fibre filter paper or silicone gel. Each collection sample is exposed over a 50 m to 5 km height range with a total of 45 separate ranges. Post-flight electron microscopy gives size-resolved information on particle number, shape and elemental composition. Each collection probe is equipped with a suite of sensors to capture the probe's status during the fall. Parachute recovery systems along with GPS-based localization ensure that each probe can be located and recovered for post-flight analysis.

1 Introduction

The characterization of middle-atmospheric aerosols and related processes are of primary importance to investigate their influence on climate variability. The stratospheric aerosol is dominated by sub-micrometer hydrate sulfuric acid droplets which scatter incident sunlight. Sulfuric acid droplets are formed through oxidation of gases containing sulfur and sulfur dioxide (Hamill et al., 1997). The stratospheric aerosol layer extends from the tropopause to about 30 km altitude and is strongly influenced by the input of large volcanic eruptions (Bourassa et al., 2012 and Solomon et al., 2011).

Information about the size range and the concentration of stratospheric aerosols together with their vertical distribution was first obtained from balloon-borne impactor measurements in the late 1950s (Junge et al., 1961). Long-term measurements using balloon-borne particle counters (Deshler et al., 2003; Hofmann, 1990; Hofmann and Rosen, 1980; Hofmann et al., 1975) and lidar (DeFoor et al., 1992; Osborn et al., 1995; Jager, 2005) at a limited number of ground sites began in the early 1970s. Satellite

AMTD
5, 8161–8187, 2012

remote sensing observations have been carried out since the late 1970s (e.g. Stratospheric Aerosol Measurements (SAM) II from 1979 to 1991 (Pepin et al., 1997; Poole and Pitts, 1994), Stratospheric Aerosol and Gas Experiment (SAGE) from 1979–1981, SAGE II from 1984 to 2005 (McCormick et al., 1979) and SAGE III from 2001 to present (Thomason et al., 2007)).

The upper-mesosphere aerosol is dominated by meteoric material that enters the Earth's atmosphere, ablates, and forms nanometer-sized aerosol particles through chemical conversion, re-condensation, and coagulation. These particles are important for middle-atmospheric processes, such as noctilucent clouds (NLCs), polar mesospheric summer echoes (PMSEs), metal layers, and the heterogeneous chemistry that controls the budget of key species like water vapour (Turco et al., 1982; Summers and Siskind, 1999; Plan, 2000; Megner et al., 2008).

Information on the spatial extent and abundance of NLCs and PMSEs as well as the size and composition of NLC particles are continuously monitored by satellite-based instruments (e.g. Deland et al., 2006; Pérot et al., 2010) and ground-based instruments since the late 1970s (e.g. Bremer et al., 2009; Kaifler et al., 2011). On the other hand, the microphysical properties of meteoric-smoke particle are still poorly understood. This lack of knowledge is due to the complications involved with in-situ measurements at mesospheric altitudes that can only be reached by sounding rockets (Havnes et al., 1996; Goldberg et al., 2001; Smiley et al., 2002; Rapp et al., 2005; Lynch et al., 2005; Hedin et al., 2007b). Furthermore, the detection of nanometer sized particles is constrained by the shock wave in front of the rocket which may prevent small particles from reaching the detector (Hedin et al., 2007a) and by contamination from the rocket itself. Hence, reliable in-situ aerosol measurements in the middle atmosphere are rare. Note that balloon-borne in-situ measurements only reach heights of up to 30 km while rocket-borne in-situ measurements only cover the upper mesosphere. Therefore, a new method for in-situ sampling of middle-atmospheric aerosol particles and successive characterization of their chemical composition is needed.

AMTD
5, 8161–8187, 2012

This paper presents a novel instrument which has been developed as a proof of concept of an in-situ aerosol collection technique covering the mesosphere and stratosphere. It will be tested in the framework of the Rocket deployed Atmospheric probes conducting Independent measurements in Northern Sweden (RAIN) experiment which has been realized through participation in the REXUS/BEXUS program, a bi-lateral cooperation between the Swedish National Space Board (SNSB) and the German Aerospace Centre (DLR). RAIN is part of the REXUS-11 sounding rocket whose launch is currently scheduled for late 2012. The REXUS-11 is powered by an Improved Orion solid fuel motor. The rocket is unguided and reaches an altitude of 85 km.

This paper begins with an overview of the instrument design and the flight timeline in Sect. 2. Section 3 describes the design and testing of the Aerosol Collection Experiment (ACE). Information regarding the electronics is summarized in Sect. 4 and conclusions are provided in Sect. 5.

2 Experiment outline

The experiment consists of two main sections: a Rocket Mounted Unit (RMU) shown in Fig. 2 and the two collection probes or Free Falling Units (FFUs) shown in Fig. 3.

The RMU is a standard REXUS module (EuroLaunch, 2010) containing an FFU ejection system. The FFU ejection system is a spring based mechanism constrained by a steel cable guided around the outside of the RMU. Ejection of the FFUs occurs when a pyro cutter cuts the cable. Both FFUs are symmetrically ejected in the spin plane at $5\,m\,s^{-1}$.

Each FFU has a cylindrical shape with a height of 93 mm and a diameter of 116 mm. It is composed of a parachute recovery system, an electronics system and an Aerosol Collection Experiment (ACE). A parachute is held inside the FFU hat on top of the FFU, which is released by a spring loaded parachute deployment mechanism. The electronics system is used to power, control and monitor the FFU and is elaborated on

AMTD
5, 8161–8187, 2012

in Sect. 4. The ACE is responsible for collecting aerosol particles and is discussed in Sect. 3.

The experiment timeline starts 67 s after launch at an altitude of approximately 63 km when the FFUs are ejected from the RMU. Given that the rocket is spinning at 4 Hz at ejection, the FFUs are ejected spinning about their longitudinal axes. This rotation results in angular momentum that stabilises each FFU. The FFUs continue to rise to an apogee of approximately 85 km, 150 s after launch. At apogee, each FFU will activate its ACE. The ACE is deactivated after the FFU has fallen to an altitude of approximately 17 km, 320 s after launch. At 6 km or 360 s after launch the FFU will deploy its parachute. An alive signal along with the FFU's GPS position will begin to be broadcast at this point. FFU touchdown will occur approximately 1200 s after launch. The FFU will continue to transmit its position until the FFUs are recovered by a helicopter recovery crew or its battery expires approximately 24 h after launch. Figure 1 shows a flight timeline diagram that presents the major milestones of the experiment's flight.

The returned FFUs will have their aerosol collection samples analyzed using scanning electron microscopy (SEM). SEM analysis gives information about size, form, and composition of the collected particles. At present, electron microscopy is the only method used to investigate these parameters down to a particle diameter of 15 nm (Kandler et al., 2007; Capannelli et al., 2011). SEM used for the investigation of aerosol particles has been used for more than 50 yr (e.g. Parungo and Nagamoto, 1986; Sielicki et al., 2011).

3 Aerosol Collection Experiment

The Aerosol Collection Experiment (ACE) is located in the base of an FFU as shown in Fig. 3. The ACE system includes a group of aerosol collection samples held inside a collection plate assembly. During the FFU's fall, aerosol particles are captured as they collide with collection samples that are exposed to the passing atmosphere. Exposure of individual collection samples is controlled by a stepper motor powered drive

AMTD
5, 8161–8187, 2012

system shown in Fig. 4. The drive system rotates the collection plate containing the collection samples past an arrangement of exposure windows in the base of the FFU. The position of the collection plate is monitored by a magnetic angular encoder. This way, each collection sample's angular position on the plate can be matched with a time and altitude range of sampling. An FFU's altitude is extracted from GPS data collected throughout the FFU's fall. Timing data is provided by the internal FFU clock.

3.1 Assembly

The collection plate assembly has three components: the aerosol collection sample holders, the collection plate lid, and the collection plate. An exploded view of the assembly is shown in Fig. 5.

There are a total of 110 aerosol collection samples inside an FFU. Each sample is 3 mm in diameter and is made from one of three separate materials. There are 44 copper grid coated carbon film collection samples that are typically used in transmission electron microscopy (TEM) applications. Each of these samples is 0.01 mm thick. There are three sub-types of these samples: 18 Formvar/Carbon 400 mesh samples with a grid hole size of 42 µm, 16 Ultrathin Carbon Type-A, 400 mesh samples and 10 Ultrathin Carbon Film on Holey Carbon Support Film, 400 mesh. These TEM grids are manufactured by Ted Pella, Inc., USA. The sticking probability for nanometre particles accelerated to 1 km s^{-1} on TEM grids was tested by Reissaus et al. (2006). Furthermore, Reissaus et al. (2006) found that nanoparticles (composed of Al_2O_3 and carbon), both as single particles and fractal agglomerates, do stick after impacts at high velocities with moderate to high efficiency (10–90 %) to these targets. An additional 22 collection samples are 0.3 mm thick pieces of glass fibre filter (PreSep TCLP Filter, glass fibre, 0.5 µm, Advance Scientific and Chemical, Inc., USA). The remaining 44 collection samples are 20 µl drops of silicone gel (NuSil Silicone Technology, USA, gel-8100).

The various aerosol collection samples have been chosen based on the size of particles they are expected to collect. The Ultrathin Carbon Film on Holey Carbon grids (red

AMTD
5, 8161–8187, 2012

material type in Fig. 6) are expected to collect mesospheric particles with diameters in the range between 5 and 20 nm. They are therefore positioned on the collection plate so that they will be exposed while the FFU is falling through the mesosphere, where nanometer sized meteoric smoke particles may be collected. The remaining copper grid coated carbon film samples are expected to collect particles with sizes on the order of tens to hundreds of nanometers. The glass fibre filters and gels are expected to collect particles up to micrometer sizes.

The arrangement of the collection samples inside a collection plate assembly is shown in Fig. 6. The row 1 and 6 collection samples are not exposed during the fall. These are control samples that will be analyzed to check for sample contamination. Rows 2, 3, 4 and 5 all house samples that will be exposed.

Each collection sample is placed inside a 3 mm diameter bed cut into the surface of a 5 mm high and 12 mm diameter collection sample holder. The beds are arranged in a pattern that matches the shape of the exposure windows in the base of the FFU. The holder has been designed to have the same dimensions as a sample holder typically used in SEM. To observe the collection samples during post-flight analysis, the sample holder is taken out of the experiment and put directly into the microscope, preventing possible contamination.

The collection plate shown in Fig. 5 is a modified 90 mm diameter and 5 mm tall spur gear. The collection plate has 22 beds that are 3 mm high and 12 mm in diameter cut out of its bottom surface to house 22 collection sample holders. The collection plate is attached to a central shaft about which the plate rotates. A collection plate lid is fastened to the collection plate after the sample holders have been loaded. The lid, shown in Fig. 5, has a mirror pattern of 2 mm high and 12 mm diameter beds to the collection plate, which the protruding sections of the collection sample holders rest in, thereby securing the holders in the collection plate assembly.

Below the collection plate assembly is the FFU base plate. The collection samples are exposed to the passing atmosphere through two exposure windows in the plate shown in Fig. 7. The outer window exposes the set of collection sample holders in rows

AMTD
5, 8161–8187, 2012

2 and 3, while the inner window exposes samples in rows 4 and 5. One, three or five collection samples are exposed at any one time during the rotation of the collection plate.

To ensure that the collection samples are not contaminated inside the structure a seal is created between the collection plate and the base plate using teflon coated glass fibre covers. One cover is glued onto the top surface of the base plate while the other is glued to the bottom surface of the collection plate assembly. The two surfaces are pressed together by a spring washer positioned on the central shaft between the top of the collection plate and the ceiling of the FFU's ACE compartment.

3.2 Actuation and control

The ACE is driven by a Faulhaber AM1020 stepper motor with a Faulhaber 10/1 256:1 gearhead. The motor/gearhead is geared down further by a 216:5 gear system resulting in a total gear ratio of 55 296:5. The motor is operated at 3857 rpm corresponding to a collection plate rotation rate of 0.39 rpm.

A control procedure rotates the stepper motor at a continuous speed, checks for stalling and attempts to recover rotation in case of a stall. The magnetic angular encoder above the collection plate's central shaft tracks a magnet on the shaft tip. If the magnet ceases to rotate for 0.1 s during the collection phase of the experiment it is assumed that the motor has stalled. After a 0.1 s delay the motor is restarted with maximum current for 5 s, after which the motor current is returned to nominal levels to avoid motor winding burnout. The maximum winding current results in a 50 % increase in nominal motor torque. When the angular encoder measures that the collection plate has been rotated a full 360° after 170 s of rotation, the collection phase has come to an end and the motor is deactivated.

AMTD
5, 8161–8187, 2012

3.3 Collection regime

The scientific goal of RAIN is to collect aerosol particles over a large altitude range, and to be able to compare the composition of aerosol particles at different heights between 85 km and 17 km. The height range studied is divided into 45 separate ranges, given that 45 out of the 48 columns shown in Fig. 6 contain collection samples. The remaining three columns expose sections of the collection plate without collection samples before the FFU starts to fall and after the collection regime is complete.

The time required for the FFU to fall through the entire height range of interest is approximately 170 s. Operating the motor at 3857 rpm for this period of time allows for each collection plate column to be passed by the exposure windows. Figure 8 shows the resulting height ranges that each column in row 2 is exposed to during the fall.

Each collection sample row differs in their respective sample exposure times based on the size of the exposure window and the sample's radial distance from the centre of the collection plate. Table 1 shows how long a single sample in a given row is exposed for. During post-flight analysis plate angular position is matched with GPS altitude data.

3.4 Particle collection and contamination testing

Two different tests were conducted to check for contamination effects. First, a laboratory test was performed to ensure that no contamination was caused by the instrument itself. In a second test under atmospheric conditions parts of the sample holders were exposed to the environment. The used target materials were checked by SEM (JOEL JSM-7401F) before every test run and images were taken from selected sample quadrants for a later comparison to post-sampling conditions.

For the first test, a sample holder loaded with one TEM grid, one glass fibre filter, and one silicone gel sample were loaded into the collection plate and one full plate rotation was performed. SEM analysis was performed directly after the test. While the analysis of the TEM grid and the silicone gel sample showed no signs of contamination, two kinds of particles were found on the glass fibre filter. Analysis of the latter filter revealed

AMTD
5, 8161–8187, 2012

that one particle was a 200 µm long fibre originating most likely from the teflon and glass fibre covers between the aerosol collection plate and the baseplate. The other particles were aluminium based between 0.15 and 0.25 µm in diameter. These kind of particles were most likely from the FFU aluminium structure. The chemical composition of the particles are given in Table 2 as Spectra 1 and 2.

For the atmospheric test the FFU was loaded with seven sample holders: four TEM grids, one glass fibre filter sample and two silicone gel samples. The loaded FFU was exposed to the atmosphere at around 90 km h^{-1} on the E4 highway, north of Stockholm on 29 November 2011. During this test the rotating collection plate exposed five samples for 10 s each. The one control TEM grid that was not exposed to the atmosphere did not show particle contamination. Particles with sizes between 100 nm 10 µm were found on the TEM and glass fibre filter. The results of X-ray analysis of these particles are given in Table 2 as Spectrum 3. Particles with diameters between 100 nm and 50 µm were found on the glass fibre filter (Fig. 9a) and silicone gel samples. Figure 9b shows a particle of the size of around 5 µm found on a TEM grid. These particles were most likely road salt, containing Na, Cl, F, and K and asphalt particles containing Ca, O, and C or Si, O, and C. The mean X-ray analysis spectrum from salt-containing particles is given as Spectrum 4 in Table 2.

4 Electronics

The experiment electronics is split between the FFUs and the RMU. The experiment is fully automated during launch. The ejection of the FFUs is a timed event, and after leaving the rocket the FFUs activate their ACEs, collect sensor data, deploy their parachutes and transmit localization messages based on a predetermined timeline hardcoded in the on-board ProASIC3 Finite Programmable Gate Arrays (FPGAs) from Actel. Each FFU has a Main FPGA responsible for monitoring the flight schedule and activating events and a second Experiment FPGA that manages ACE control and the collection of raw GPS data.

AMTD
5, 8161–8187, 2012

Each FFU is powered by a Li-ion rechargeable SAFT MP144350 battery, which can be recharged while the FFUs are in the rocket. The nominal capacity of the battery operating at −30 °C is 2.25 Ah at a cell voltage of 2.75 V when drawing 0.5 A (Saf, 2009), which is sufficient for powering the FFU for 24 hours. This has also been proven in FFU thermal tests.

Each FFU collects and stores housekeeping and raw GPS data in a non-volatile memory sensor. From the raw GPS data it is possible to extract the position, velocity and acceleration after post processing. The internal sensors in each FFU are a LIS344ALH 3-axis accelerometer from STMicroelectronics, a LYPR540AH 3-axis angular rate sensor from STMicroelectronics, a MPXH6115A6U pressure sensor from Freescale Semiconductor, an AD590 temperature sensor from Analog Devices and the ACE AM4096D02 angular magnetic encoder from RLS. The sensor outputs are all analog and converted by AD7276 12-bit analog to digital converters (ADCs). A 16-channel multiplexer CD4067B from Texas Instruments rotates ADC input, which is sampled at 4000 samples/second. Thus each channel is sampled at 250 samples/second. The Main FPGA packages the ADC data with a time stamp and saves it into a HY27UF(08/16)4G2B 4 Gbit NAND memory from Hynix.

The raw GPS data is collected using a consumer grade MAX2769 front end from Maxim. An active WS3914 antenna from Wi-Sys Communications provides the signal to the input of the front end, which down converts and digitizes the data in a 2-bit sign/magnitude format at 8.192 Msamples/second. The intermediate frequency is set to 1575.42 MHz. The recorded raw data are analyzed post-flight using a software GPS receiver and a custom trajectory reconstruction algorithm. The use of raw data recording is in part to circumvent the altitude and speed limitations imposed on commercial GPS modules, and in part to improve the trajectory reconstruction accuracy.

Upon parachute deployment, the localization system is activated. The GPS antenna signal is re-routed by a PE4230 RF switch from Peregrine Semiconductor to an ET-318 commercial GPS module from US Global Sat.

AMTD
5, 8161–8187, 2012

The GPS coordinates are modulated into a radio beacon signal transmitted using the radio beacon antenna. Each FFU transmits this signal on a distinct frequency, either 173.225 MHz or 172.250 MHz. The GPS coordinates are also transmitted to the Globalstar satellite network via the satellite modem and antenna.

The RMU houses communication relay circuitry that allows ground controllers to command each FFU and activate the camera on board the RMU, which has a view out the side of the rocket cylinder and captures the entire rocket flight. All communication with the RMU passes through the REXUS service module described in (EuroLaunch, 2010). Power is supplied to the RMU and FFUs while they are still in the rocket by the rocket's service module's batteries. Ejection of the FFUs is not controlled by RMU circuitry, it is triggered directly by a mechanical timer in the service module.

5 Conclusions

The proposed technique is a new method for collecting aerosol particles in the mesosphere and stratosphere that have previously been inaccessible to balloon and sounding rocket aerosol collection experiments. Two collection probes or FFUs ejected from the sides of a sounding rocket collect aerosol particles between 85 and 17 km. Each FFU incrementally exposes collection samples to the passing atmosphere over 45 separate height ranges.

Three separate types of sample materials are used to collect particles of different size ranges. On the TEM grids it is expected that meteoric smoke particles in the size range between 5 and 10 nm in the mesosphere and larger than 10 nm in the stratosphere (Megner et al., 2006, 2008) be sampled. As shown by (Hedin et al., 2007a) however, the detection efficiency for meteoric-smoke particles in the nanometre size range is very much altitude dependent. Hedin et al. (2007a) also mentioned that below 70–75 km it is difficult to detect any particles smaller than 5 nm. Particles are expected to be larger at lower altitudes (Megner et al., 2006). It is expected that the larger stratospheric aerosol particles be sampled on the glass fibre and silicone gel.

AMTD
5, 8161–8187, 2012

After collecting aerosols, each FFU broadcasts its GPS position and is recovered by a ground support crew. SEM and X-ray analysis of each collection sample is performed after recovery. The technique has been proven to not significantly contaminate the collection samples during handling and the running of the experiment. It has also been shown that aerosol particles as small as 100 nm have been observed after exposure to an aerosol rich environment when travelling at 90 km h^{-1}.

Acknowledgements. We would like to thank the entire RAIN team for their hard work and commitment to the design, implementation and testing of the experiment. Thanks goes to the Swedish National Space Board for their support throughout the development of this experiment. Thanks to the Swedish National Space Board and German Aerospace Centre for organizing and managing the REXUS project, without which launch of the experiment would not be possible. The department of Space and Plasma Physics and the department of Mechanics at KTH have been invaluable with providing continued help and support. We would also like to acknowledge Lars Jansson and Sofhia Josborg for their help with the scanning electron microscope analysis.

References

Bourassa, A., Robock, A., Randel, W., Deshler, T., Rieger, L., Lloyd, N., Llewellyn, E., and Degenstein, D.: Large Volcanic Aerosol Load in the Stratosphere Linked to Asian Monsoon Transport, Science, 337, 78–81, 2012. 8162

Bremer, J., Hoffmann, P., Latteck, R., Singer, W., and Zecha, M.: Long-term changes of (polar) mesosphere summer echoes, J. Atmos. Sol-Terr. Phy., 71, 1571–1576, 2009. 8163

Capannelli, G., Castello, E., Comite, A., Costa, C., and Mamolini, G.: Electron microscopy characterization of airborne micro- and nanoparticulate matter, J. Electron Microsc., 60, 117–131, 2011. 8165

DeFoor, J., Robinson, E., and Ryan, S.: Early lidar measurements of the June 1991 Pinatubo eruption plume at Manua Loa Observatory, Geophys. Res. Lett., 19, 187–190, 1992. 8162

DeLand, M. T., Shettle, E. P., Thomas, G. E., and Olivero, J. J.: A quarter-century of satellite PMC observations, J. Atmos. Sol-Terr. Phy., 68, 9–29, 2006. 8163

AMTD

5, 8161–8187, 2012

Deshler, T., Hervig, M., Hofmann, D., Rosen, J., and Liley, J.: Thirty years of in situ stratospheric aerosol size distribution measurements from Laramie, Wyoming (41° N), using balloon-borne instruments, J. Geophys. Res., 108, D22, doi:10.1029/2002JD002514, 2003. 8162

EuroLaunch: REXUS User Manual, Euro Launch, 7.1st Edn., available at: http://www.rexusbexus.net/index.php?option=com_content&view=article&id=47&Itemid=59 (last access: 7 May 2011), 2010. 8164, 8172

Goldberg, R., Pfaff, R., Holzworth, R., Schmidlin, F., Voss, H., Tuzzolino, A., Croskey, C., Mitchell, J., Friedrich, M., Murtagh, D., Witt, G., Gumbel, J., von Zahn, U., Singer, W., and Hoppe, U.: DROPPS: a study of the polar summer mesosphere with rocket, radar and lidar, Geophys. Res. Lett., 28, 1407–1410, 2001. 8163

Hamill, P., Jensen, E., Russell, P., and Bauman, J.: The Life Cycle of Stratospheric Aerosol Particles, B. Am. Meteorol. Soc., 78, 1395–1410, 1997. 8162

Havnes, O., Troim, J., Blix, T., Mortensen, W., Naesheim, L., Thrane, E., and Tonnesen, T.: First detection of charged dust in the Earthatmosphere, J. Geophys. Res., 101, 10839–10847, 1996. 8163

Hedin, J., Gumbel, J., and Rapp, M.: On the efficiency of rocket-borne particle detection in the mesosphere, Atmos. Chem. Phys., 7, 3701–3711, doi:10.5194/acp-7-3701-2007, 2007a. 8163, 8172

Hedin, J., Gumbel, J., Waldemarsson, T., and Giovane, F.: The aerodynamics of the MAGIC meteoric smoke sampler, Adv. Space Res., 40, 818–824, doi:10.1016/j.asr.2007.06.046, 2007b. 8163

Hofmann, D.: Increase in the stratospheric background sulfuric acid aerosol mass in the past 10 years, Science, 248, 996–1000, 1990. 8162

Hofmann, D. and Rosen, J. M.: Stratospheric sulfuric acid layer Evidence for an anthropogenic component, Science, 208, 1368–1370, 1980. 8162

Hofmann, D., Rosen, J. M., Pepin, T. J., and Pinnick, R. G.: Stratospheric aerosol measurements I, Time variations at northern midlatitudes, J. Atmos. Sci., 32, 1446–1456, 1975. 8162

Jager, H.: Long-term record of lidar observations of the stratospheric aerosol layer at Garmisch-Partenkirchen, J. Geophys. Res., 110, D08106, doi:10.1029/2004JD005506, 2005. 8162

Junge, C., Changnon, C., and Manson, J.: A world-wide stratospheric aerosol layer, Science, 133, 1478–1479, 1961. 8162

Kaifler, N., Baumgarten, G., Fiedler, J., Latteck, R., Lübken, F.-J., and Rapp, M.: Coincident measurements of PMSE and NLC above ALOMAR (69° N, 16° E) by radar and lidar from

AMTD
5, 8161–8187, 2012

1999–2008, Atmos. Chem. Phys., 11, 1355–1366, doi:10.5194/acp-11-1355-2011, 2011. 8163

Kandler, K., Benker, N., Bundke, U., Cuevas, E., Ebert, M., Knippertz, P., Rodriguez, S., and Weinbruch, L. S. S.: Chemical composition and complex refractive index of Saharan Mineral Dust at Izana, Tenerife (Spain) derived by electron microscopy, Atmos. Environ., 41, 8058–8074, 2007. 8165

Lynch, K. A., Gelinas, L., Kelley, M., Collins, R., Widholm, M., Rau, D., MacDonald, E., Liu, Y., Ulwick, J., and Mace, P.: Multiple sounding rocket observations of charged dust in the polar winter mesosphere, J. Geophys. Res., 110, A03302, doi:10.1029/2004JA010502, 2005. 8163

McCormick, M., Hamill, P., Pepin, T. J., Chu, W. P., Swissler, T. J., and McMaster, L. R.: Satellite studies of the stratospheric aerosol, B. Am. Meteorol. Soc., 60, 1038–1046, 1979. 8163

Megner, L., Rapp, M., and Gumbel, J.: Distribution of meteoric smoke – sensitivity to microphysical properties and atmospheric conditions, Atmos. Chem. Phys., 6, 4415–4426, doi:10.5194/acp-6-4415-2006, 2006. 8172

Megner, L., Siskind, D., Rapp, M., and Gumbel, J.: Global and temporal distribution of meteoric smoke: A two-dimensional simulation study, J. Geophys. Res., 113, D03202, doi:10.1029/2007JD009054, 2008. 8163, 8172

Osborn, M., DeCoursey, R. J., Trepte, C. R., Winder, D. M., and Woods, D. C.: Evolution of the Pinatubo volcanic cloud over Hampton Virginia, Geophys. Res. Lett., 22, 1101–1104, 1995. 8162

Parungo, F. and Nagamoto, C.: Temporal and spatial variations of marine aerosols over the Atlantic Ocean, Atmos. Res., 20, 23–37, 1986. 8165

Pepin, T., McCormick, M. P., Chu, W. P., Simon, F., Swissler, T. J., Adams, R. R., Crumbly, K. R., and Fuller, W. H.: Stratospheric aerosol measurements, NASA Spec. Publ., SP-421, 127–136, 1997. 8163

Pérot, K., Hauchecorne, A., Montmessin, F., Bertaux, J.-L., Blanot, L., Dalaudier, F., Fussen, D., and Kyrölä, E.: First climatology of polar mesospheric clouds from GOMOS/ENVISAT stellar occultation instrument, Atmos. Chem. Phys., 10, 2723–2735, doi:10.5194/acp-10-2723-2010, 2010. 8163

Plan, J.: The role of sodium bicarbonate in the nucleation of noctilucent clouds, Ann. Geophys., 18, 807–814, 2000, http://www.ann-geophys.net/18/807/2000/. 8163

AMTD
5, 8161–8187, 2012

Poole, L. and Pitts, M. C.: Polar stratospheric cloud climatology based on Stratospheric Aerosol Measurement II observations from 1978 to 1989, J. Geophys. Res., 99, 13083–13089, 1994. 8163

Rapp, M., Hedin, J., Strelnikova, I., Friedrich, M., Gumbel, J., and Lübken, F.-J.: Observations of positively charged nanoparticles in the nighttime polar mesosphere, Geophys. Res. Lett., 32, L23821, doi:10.1029/2005GL024676, 2005. 8163

Reissaus, P., Waldemarsson, T., Blum, J., Clement, D., Llamas, I., Mutschke, H., and Giovane, F.: Sticking efficiency of nanoparticles in high-velocity collisions with various target materials, J. Nanopart. Res., 8, 693–703, 2006. 8166

SAFT: Rechargeable Li-ion battery; MP 144350, available at: http://www.saftbatteries.com/doc/Documents/liion/Cube572/MP144350_1009.ff6efb8d-6aab-45ef-ae7a-7fe4af5b011d.pdf (last access: 4 September 2012), 2009. 8171

Sielicki, P., Janik, H., Guzman, A., and Namiesnik, J.: The Progress in Electron Microscopy Studies of Particulate Matters to Be Used as a Standard Monitoring Method for Air Dust Pollution, Cr. Rev. Anal. Chem., 41, 314–334, 2011. 8165

Smiley, B., Rapp, M., Blix, T., Robertson, S., Horanyi, M., Latteck, R., and Fiedler, J.: Charge and size distribution of mesospheric aerosol particles measured inside NLC and PMSE during MIDAS MaCWAVE, J. Atmos. Sol.-Terr. Phys., 68, 114–123, 2002. 8163

Solomon, S., Daniel, J. S., III, R. N., Vernier, J.-P., Dutton, E., and Thomason, L.: The Persistently Variable Background Stratospheric Aerosol Layer and Global Climate Change, Science, 333, 886–870, 2011. 8162

Summers, M. E. and Siskind, D. E.: Surface recombination of O and H_2 on meteoric dust as a source of mesospheric water vapor, Geophys. Res. Lett., 26, 1837–1840, 1999. 8163

Thomason, L. W., Poole, L. R., and Randall, C. E.: SAGE III aerosol extinction validation in the Arctic winter: comparisons with SAGE II and POAM III, Atmos. Chem. Phys., 7, 1423–1433, doi:10.5194/acp-7-1423-2007, 2007. 8163

Turco, R., Toon, O., Whitten, R., Keesee, R., and Hollenbach, D.: Noctilucent clouds: Simulation studies of their genesis, properties and global influences, Planet. Space Sci., 3, 1147–1181, 1982. 8163

AMTD
5, 8161–8187, 2012

Table 1. The aerosol collection sample exposure times associated with each row of samples on the collection plate as shown in Fig. 6. Collection samples are exposed as the collection plate is rotated past the exposure windows in the base of the FFU. The exposure times vary based on the radial position of each row. Rows 1 and 6 as indicated in Fig. 6 hold control samples and are not exposed to the atmosphere.

Row	Exposure Time [s]
1	0.0
2	4.0
3	1.7
4	2.3
5	2.7
6	0.0

AMTD
5, 8161–8187, 2012

Table 2. Mean results of the X-ray analysis of particles measured during the sampling tests. Spectra 1 and 2 show the mean of two and four individual analyses of particles found after the laboratory test, respectively. Spectra 3 and 4 each show the mean of two x-ray analyses of particles found during the atmospheric test.

	C	N	O	Al	Cl	Pd	Si	F	Ca
Spectrum 1	–	17	58	19	6	–	–	–	
Spectrum 2	–	–	27	72	–	–	–	–	
Spectrum 3	83	–	17	–	–	–	–	–	
Spectrum 4	24	–	18	2	–	–	15	32	3

AMTD
5, 8161–8187, 2012

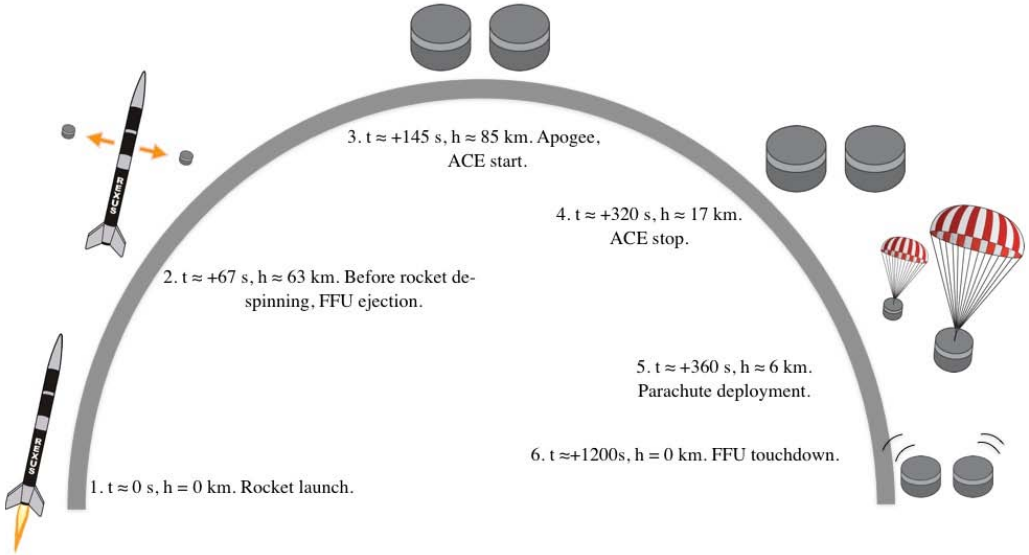

Fig. 1. The major milestones of the RAIN experiment include launch, ejection of the FFUs from the rocket, Aerosol Collection Experiment deactivation, initiation, Aerosol Collection Experiment parachute deployment, localization system initiation and FFU touchdown.

AMTD
5, 8161–8187, 2012

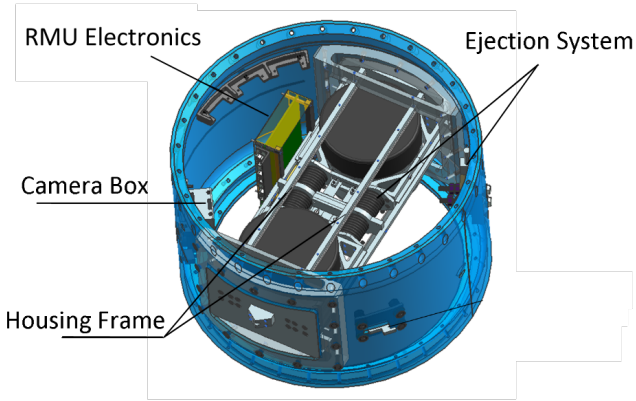

Fig. 2. The Rocket Mounted Unit (RMU). A modified REXUS rocket cylinder that houses the Free Falling Units (FFUs), the FFU ejection system and the RMU electronics. The ejection system pushes the FFUs out the sides of the rocket 67 s after launch. The electronics are used to control communication between the FFUs, the RMU and the REXUS Service Module. In addition a camera is mounted on the inner wall of the RMU looking outwards to capture footage of the REXUS flight.

AMTD
5, 8161–8187, 2012

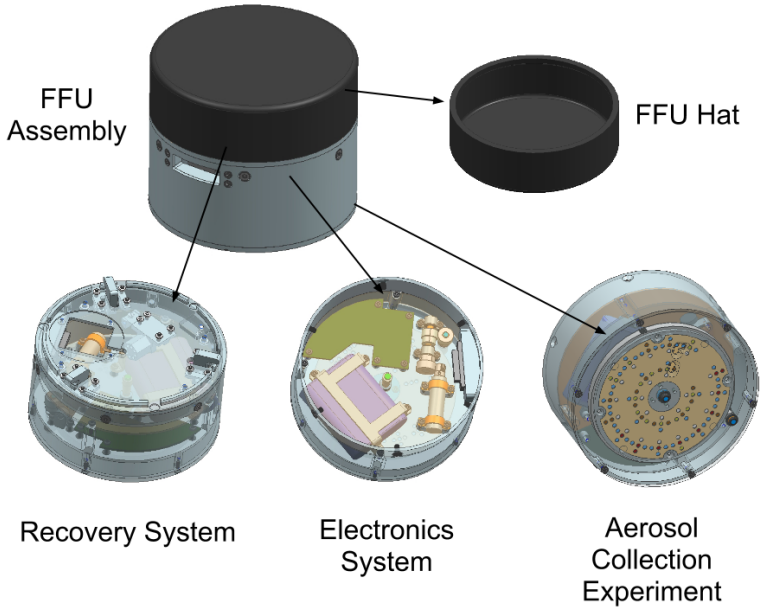

Fig. 3. The FFU is divided into four parts. The FFU hat holds a parachute inside it. The hat and parachute are deployed by the recovery system when the FFU falls past an altitude of 6 km. The electronics system is responsible for running the collection experiment, recording sensor readings and transmitting localization signals.The Aerosol Collection Experiment exposes 3 mm diameter collection samples to the passing atmosphere between altitudes of 85 and 17 km.

AMTD
5, 8161–8187, 2012

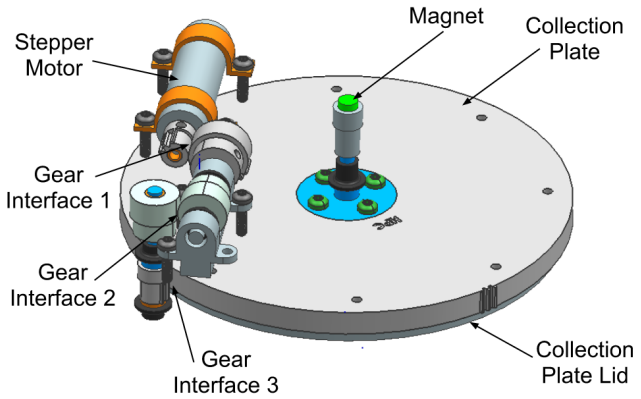

Fig. 4. The Aerosol Collection Experiment (ACE) is composed of the collection plate assembly which is rotated in the base of the FFU to incrementally expose aerosol collection samples to the passing atmosphere. The stepper motor drives the collection plate via the gear system. A magnet on the central shaft of the collection plate assembly is used with a magnetic angular encoder to track the angular position of the ACE.

AMTD
5, 8161–8187, 2012

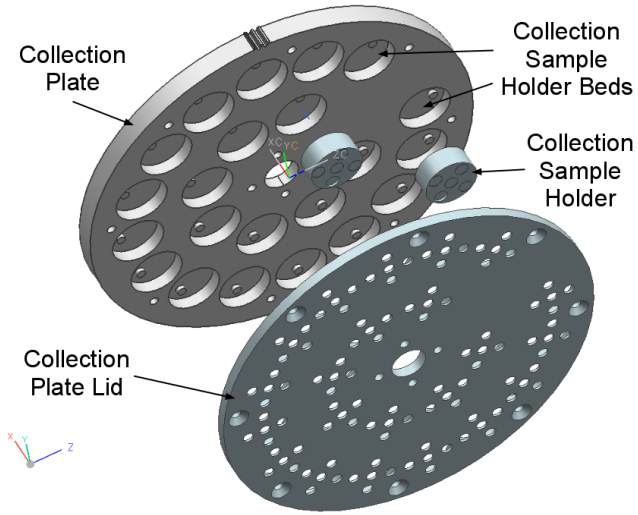

Fig. 5. The collection plate assembly is composed of a collection plate, which holds 22 collection sample holders inside its collection sample holder beds. The collection plate lid is fastened to the collection plate to hold the collection sample holders in place.

AMTD
5, 8161–8187, 2012

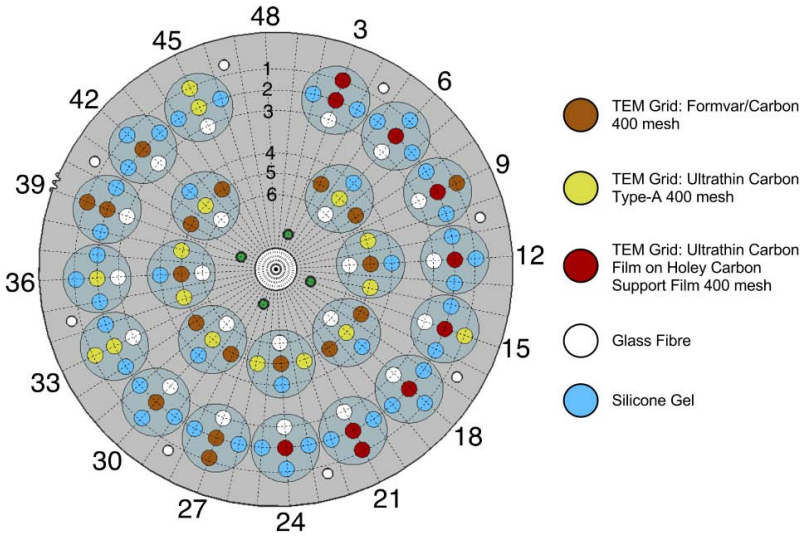

Fig. 6. The coordinate system for the positioning of each of the aerosol collection samples. Six rows and 48 columns are used to locate specific collection samples. The columns are on the radial lines originating at the centre of the collection plate and the rows are the concentric circles. Each collection sample is colour coded to indicate the sample's material type.

AMTD
5, 8161–8187, 2012

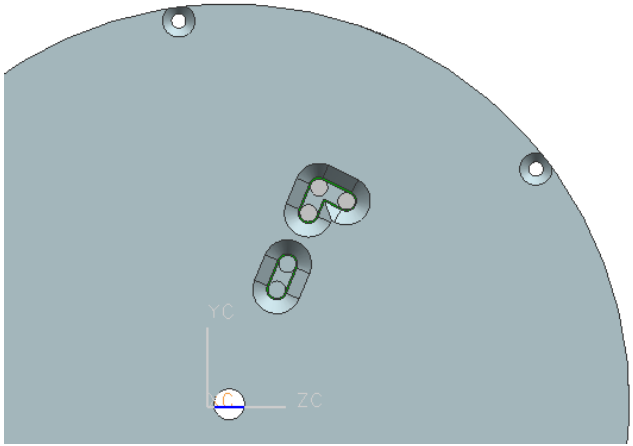

Fig. 7. Two exposure windows in the base plate allow for aerosol collection samples to be exposed to the passing atmosphere during the FFU's fall. Collection samples are incrementally passed by these windows throughout the fall. A maximum of three and two collection samples can be exposed through the top and bottom windows respectively at any one time.

AMTD
5, 8161–8187, 2012

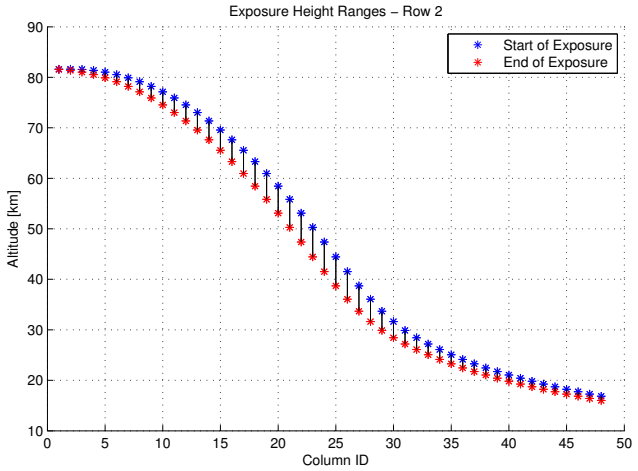

Fig. 8. The height ranges that each of the collection samples in row 2 from Fig. 6 are exposed to according to a six degree of freedom simulation of a falling FFU. There are 45 distinct height ranges that samples are exposed to.

AMTD
5, 8161–8187, 2012

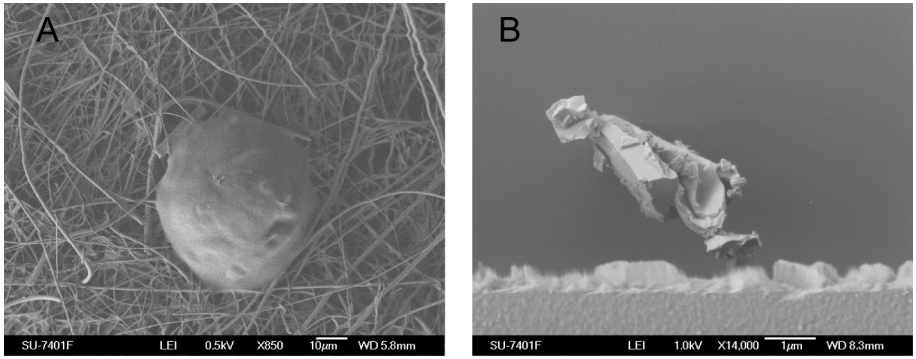

Fig. 9. A particle with a size of around 50 µm found on glass fibre filter **(A)** after the car test. **(B)** shows a 5 µm sized particle found on a TEM grid. During the test the collection sample was exposed to a 90 km h^{-1} air flow.

AMTD
5, 8161–8187, 2012